A Heterodyne Scanning System for Hologram Transmission†

By ARTHUR B. LARSEN

(Manuscript received November 19, 1968)

This paper describes the experimental realization of a recently proposed scanning reference beam technique for hologram transmission. The apparatus uses an extremely simple method for obtaining the two different but phase-locked optical frequencies necessary for the heterodyne mode of operation. The paper shows reconstructions obtained from transmitted holograms of two- and three-dimensional objects, analyzes the signal-to-noise ratio and resolution attainable with this technique, derives a new general theorem concerning the detectability of the interference between two arbitrary beams, and discusses the theorem's applications to this system.

I. INTRODUCTION

The transmission of holograms over electrical channels is of interest not only because of the three-dimensional images obtainable with such a system but also because of the possible advantages of the holographic process as a coding technique for subjectively more error-resistant transmission of two-dimensional material. Indeed, the transmission of thin holograms over conventional television systems presents no conceptual difficulties and has already been demonstrated with low resolution holograms.[1] However, the necessity of resolving the holographic carrier fringes, as well as other unnecessary spatial frequency components, results in the waste of ¾ of the resolution capability of the camera. Although recently devised techniques can avoid this waste, the use of these techniques in useful holographic transmission systems is still limited by the resolution of camera tubes.[2]

This paper describes the experimental realization of a scanning reference beam technique for hologram transmission recently published by Enloe, Jakes, and Rubinstein.[3] This technique not only eliminates

† This paper was presented at a meeting of the Optical Society of America, Pittsburgh, October 9–12, 1968.

the camera tube but also requires minimum resolution from the optical scanner used in its place. Furthermore, the advantages of this system, because they accrue through the elimination of totally extraneous components present in all holograms, can be obtained while simultaneously using other bandwidth reduction schemes, such as those of Lin or Haines and Brumm.[4,5]

We briefly describe the system here, and give more specific apparatus information in Section IV. As Fig. 1 shows, the scanning system replaces the conventional reference beam by a focused spot which is optically scanned in a raster fashion over the surface of a large area photodetector. The detector provides an output current proportional to the integrated intensity of the total incident light. The time-varying interference between the stationary object beam and the constant amplitude scanning spot causes a variation in the detector output. This signal is amplified and transmitted electrically to a receiver, where it modulates the kinescope intensity. The hologram made by photographing the kinescope display is then used to reconstruct the original scene.

II. ANALYSIS OF HETERODYNE SCANNING

For mathematical simplicity and ease of understanding, the original analysis of the operation of this system as given by Enloe and others, was based on the assumption that the focused spot of the scanning reference beam could be represented by a delta function.[3] Actually, the reference beam cannot be focused to a mathematical point but is spread over a nonzero area. The shape and size of the limiting aperture in the system determine the nature and amount of this spreading and hence, the possible resolution. The limiting aperture in a real system is typically determined by the optical deflection system. We will here analyze the simple but practically important case of a focused spot formed from a uniform plane wave passing through a circular aperture.

Assuming the limiting aperture and center of deflection of the scanning beam to be located at the front focal point of the focusing lens, the distribution of $e_R(r, t)$, the electric field at a detector located in the rear focal plane of the lens, is given by

$$e_R(r, t) = \frac{2E_R J_1(\sigma r)}{\sigma r} \exp i(\omega_c t + \phi_R), \tag{1}$$

where $\sigma = 2\pi b/f\lambda$, b is the radius of the limiting aperture, f is the focal length of the focusing lens, r is the radial distance measured

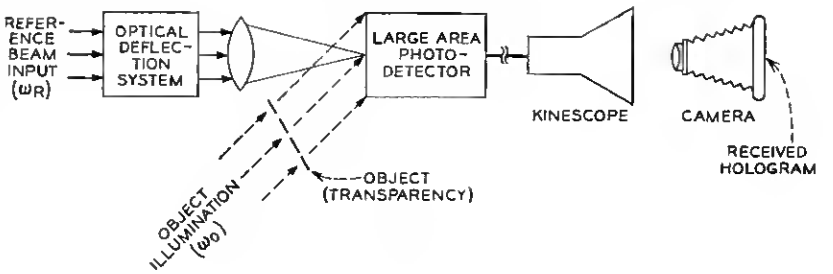

Fig. 1 — Simplified heterodyne scanning system diagram.

from the geometric center of the focused spot, and E_R, ω_R, ϕ_R, and λ are the amplitude, angular frequency, phase, and wavelength of the reference beam. The object field e_o is of the form

$$e_o(x, t) = E_o \exp i(\omega_o t + kx + \phi_o); \tag{2}$$

that is, a plane wave of amplitude E_o, angular frequency ω_o, and phase ϕ_o incident on the detector at an angle of $\theta = k\lambda/2\pi$ with respect to the normal. (Because they are virtually equal for all purposes of this derivation, no distinction is made between the wavelengths of the object and reference beams.)

With the scanning spot moving at a horizontal velocity u and a vertical velocity v, $I(r, \theta, t)$, the intensity at any point (r, θ) on the detector surface as measured from the geometric center $(x = ut, y = vt)$ of the focused spot, is given by

$$I(r, \theta, t) = |e_R(r, t) + e_o(r, t)|^2 = E_o^2 + \frac{4E_R^2 J_1^2(\sigma r)}{(\sigma r)^2} + \frac{4E_R E_o J_1(\sigma r)}{(\sigma r)}$$
$$\cdot \cos [k(ut + r \sin \theta) + (\omega_o - \omega_R)t + \phi_o - \phi_R]. \tag{3}$$

The detector output current $i(t)$ is proportional to the integral of this intensity over the detector surface of area A. Incorporating the necessary physical constants to allow writing an equality, and assuming that the detector intercepts all of the significant energy of the scanning beam so that the integrations over r can be extended to infinity, we have

$$i(t) = \frac{\eta e}{Z_o h\nu} \int I(r, \theta, t)\, dA$$
$$= \frac{\eta e}{Z_o h\nu} \left\{ E_o^2 A + \int_{r=0}^{\infty} \int_{\theta=0}^{2\pi} \frac{4E_R^2 J_1^2(\sigma r)}{(\sigma r)^2} r\, d\theta\, dr \right.$$

$$+ \int_{r=0}^{\infty} \int_{\theta=0}^{\pi} \frac{4E_R E_o J_1(\sigma r)}{\sigma r} \cos [k(ut + r \sin \theta) + (\omega_o - \omega_R)t + \phi_o - \phi_R] r \, d\theta \, dr \Bigg\}, \tag{4}$$

where η is the detector quantum efficiency, e the electronic charge, $h\nu$ the photon energy, and Z_o the impedance of free space.

The first of the two integrals in equation (4) can be evaluated by a technique outlined by Born and Wolf (see p. 398 of Ref. 6); the total dc component of the detector current then becomes

$$i_{dc} = \frac{\eta e}{Z_o h\nu} (E_o^2 A + 4\pi E_R^2/\sigma^2). \tag{5}$$

The last integral of equation (4) gives the ac (signal) component of the detector output current and can be further simplified to

$$i_s(t) = \frac{\eta e}{Z_o h\nu} \frac{8\pi E_R E_o}{\sigma} \cos [(ku + \omega_o - \omega_R)t + \phi_o - \phi_R] \cdot \int_{r=0}^{\infty} J_1(\sigma r) J_o(kr) \, dr. \tag{6}$$

Equation (6) can then be evaluated to yield[7]

$$i_s(t) = \begin{cases} \dfrac{\eta e}{Z_o h\nu} \dfrac{8\pi E_R E_o}{\sigma^2} \cos [(ku + \omega_o - \omega_R)t + \phi_o - \phi_R] \\ \qquad \text{for} \quad k < \sigma, \quad \text{that is,} \quad \theta < b/f \\ 0 \qquad \text{for} \quad k > \sigma, \quad \text{that is,} \quad \theta > b/f. \end{cases} \tag{7}$$

Thus, the scanning spot cannot resolve the phase variations in an off-axis plane wave unless $\theta < b/f$. In other words, the object beam must appear to come from witbin tbe active aperture of the lens used to form the scanning spot. Therefore, a beamsplitter of some type must be used in this system to recombine the object and reference beams.

If $\omega_o = \omega_R$, equation (7) shows the maximum electrical output frequency to be $ku/2\pi = u\theta/\lambda$. Witb a scanning system that provides a peak-to-peak angular beam deflection of Ω, the scan length in the focal plane of the scanning beam focusing lens is Ωf. At a horizontal scan velocity of u, this length will be traversed in $\Omega f/u$ seconds, during which time a maximum of $\Omega b/\lambda$ cycles will be generated. Thus, the maximum number of resolvable line pairs (or phase cbanges) is completely determined by the clear aperture and angular deflection of the optical scanner. Because the information to be modulated onto

the spatial carrier contains both positive and negative spatial frequencies, the maximum allowable modulating spatial frequency is just one-half of that determined above, giving a usable resolution of $\Omega b/2\lambda$ line-pairs per scan line. (A more detailed discussion of the resolution and bandwidth requirements for this and the following case may be found in Ref. 3.)

With $\omega_o \neq \omega_R$, equation (7) shows the ac output frequency to be limited only by $\omega_o - \omega_R$. The maximum value of k is still restricted as before, but if $\omega_o - \omega_R$ is chosen greater than uk_{max}, the entire range of k values can be used to contain a single sideband of object information, effectively doubling the scanner resolution. In this mode of operation, the transmitted holograms should yield image reconstructions having the same resolution that could be obtained by using the scanner as a flying spot image dissection system. (It may also be possible to obtain increased resolution in the case of $\omega_o = \omega_R$ by operating in a single-sideband mode; this has not yet been experimentally investigated.) The method of obtaining the two different, but phase-locked, optical frequencies needed for this maximum resolution heterodyne operation is described in Section 4.1. In both cases, the resolution in the direction parallel to the carrier fringes is determined only by the spot size.

III. SIGNAL-TO-NOISE RATIO

Under optimum conditions, the only significant noise source will be the shot noise generated in the photodetector by the dc component of the detected signal. Substituting i_{dc} as given by equation (5) into the conventional shot noise formula gives a mean-square noise current of

$$\bar{i}_n^2 = \frac{2e^2B\eta}{Z_o h\nu}\,(E_o^2 A + 4\pi E_R^2/\sigma^2), \tag{8}$$

where B is the electrical bandwidth required by the system.

Using the rms signal current as given by equation (7), the signal-to-noise (power) ratio becomes

$$\frac{\bar{i}_s^2}{\bar{i}_n^2} = \frac{32\pi^2\eta E_R^2 E_o^2}{Z_o h\nu\sigma^4 B} \Big/ \left(E_o^2 A + \frac{4\pi E_R^2}{\sigma^2}\right). \tag{9}$$

As is usual with holography, E_R and E_o will be obtained from the same laser and will thus be subject to the constraint that

$$E_o^2 A + 4\pi E_R^2/\sigma^2 \leq Z_o P_o\,, \tag{10}$$

where P_o is the laser output power. [Equation (10) states that the sum of the object and reference beam powers cannot exceed the laser power.]

It can then be shown that when $E_o^2 A = 4\pi E_R^2/\sigma^2 = \frac{1}{2} Z_o P_o$, equation (9) has a maximum given by

$$\left(\frac{\overline{i_s^2}}{\overline{i_n^2}}\right)_{\max} = \frac{4\pi\eta P_o}{B\sigma^2 A h\nu}. \tag{11}$$

Defining an equivalent scanning spot radius r_{eq} such that a field of uniform intensity E_R incident on a circular area of radius r_{eq} provides the same photodetector current as the actual incident field, we have, using the appropriate term from equation (5)

$$\pi r_{eq}^2 E_R^2 = 4\pi E_R^2/\sigma^2 \quad \text{or} \quad r_{eq} = 2/\sigma. \tag{12}$$

With N_s, the number of resolvable spots, then given approximately by $N_s = A/\pi r_{eq}^2 = A\sigma^2/4\pi$, equation (11) becomes

$$\left(\frac{\overline{i_s^2}}{\overline{i_n^2}}\right)_{\max} = \frac{\eta N_p}{B N_s}, \tag{13}$$

where $N_p = P_o/h\nu$ is the number of photons per second incident on the detector. To transmit a hologram in a specified time, B will have to be increased as N_s increases, in which case the signal-to-noise ratio decreases with the square of the number of resolvable spots.

IV. EXPERIMENTAL APPARATUS AND PRELIMINARY SYSTEM OPERATION

Figure 2 is an overall diagram of the apparatus used for the experimental verification of the heterodyne scanning system.

4.1 *Object and Reference Beam Generation*

A Spectra-Physics Model 125 50-mw He-Ne laser operating at 6328 Å is used as the optical source. The portion of its output transmitted by beamsplitter 1 is used for object illumination; the remainder is reflected at normal incidence from the moving mirror M. This introduces a Doppler shift and is the method by which the two different but phase-locked optical frequencies are obtained. The large motions required ($\approx$ 0.1 mm peak-to-peak) are readily obtained by using a modified loudspeaker assembly for the mirror driver. The Doppler-shifted light returns to the beamsplitter, where the transmitted portion proceeds to the optical deflection system.

4.2 *Beam Deflection and Focusing*

The first deflection (horizontal) is performed by an American Time Products type 44 optical scanner operating at 7.2 kHz. This unit has

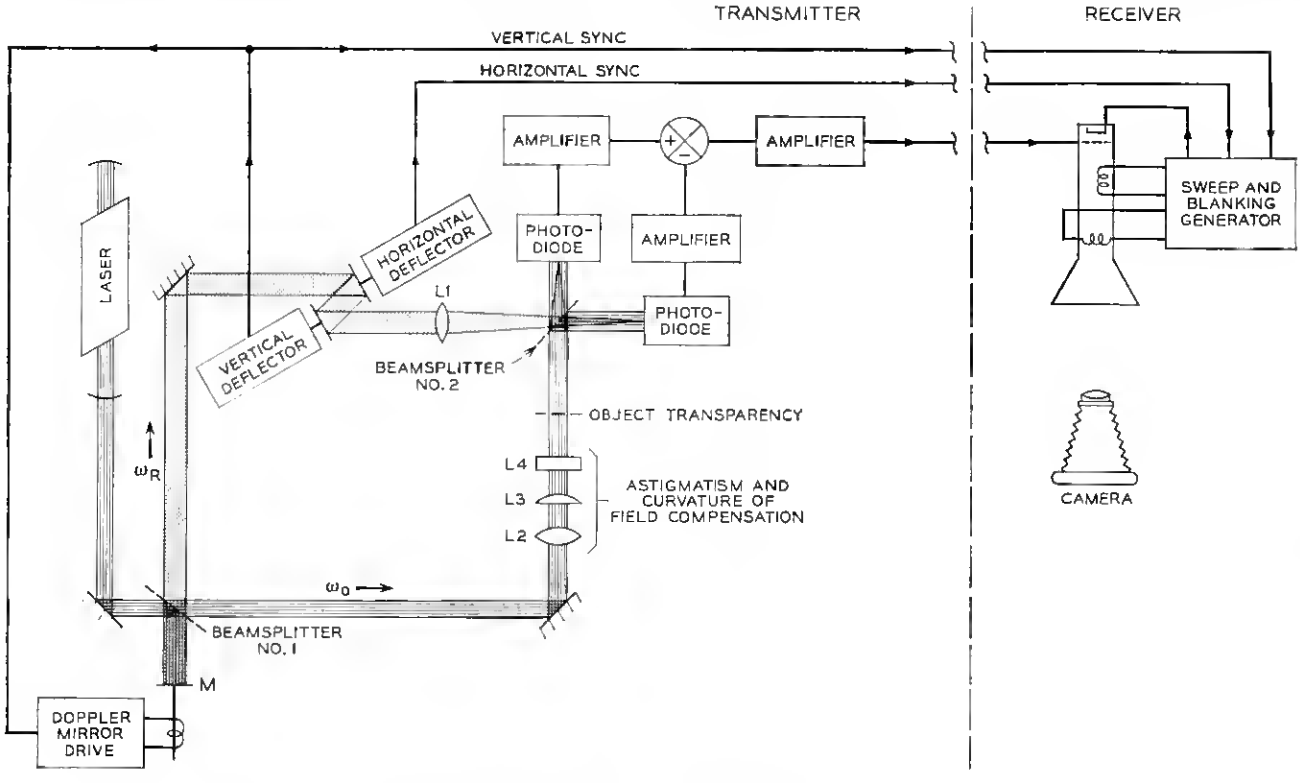

Fig. 2 — Heterodyne scanning system block diagram.

a clear aperture of 2 mm radius and provides a 6° peak-to-peak scan. The line scan thus formed is then deflected vertically by a second scanner that affords a clear aperture radius of 8 mm with a 15° peak-to-peak deflection at 60 Hz. Both scanners operate in torsional-mechanical resonance and hence provide only sinusoidal deflections.

Lens L1 transforms the angularly deflected beam into the focused scanning spot. The unavoidable physical separation of the two optical deflectors separates the horizontal and vertical centers of deflection, causing the locus of the waist of the scanning spot to be astigmatic. Compensation for this effect is provided by the inclusion of cylindrical lenses L3 and L4 in the object beam path. Spherical lens L2, in conjunction with L3 and L4, corrects for the curvature of field of the focusing lens L1 and expands the object beam to the size required to match the scanning spot raster.

4.3 *Detection*

Beamsplitter 2 is used to recombine the object and reference beams. As Section II shows, the use of a beamsplitter for this purpose is a necessity rather than a convenience. The actual detection was done using United Detector Technology type PIN-10 large area silicon photodiodes. The sensitive surface of the photodetector was originally placed at the locus of the scanning beam waist; it is still convenient to consider the detection process to occur there. However, it was experimentally observed that this particular detector location is not only unnecessary but undesirable. It is unnecessary because it can be shown that the detected beat signal is independent of the detector position provided the detector intercepts all of the area common to both beams. The special case where both beams are essentially plane waves has been long known and used by those engaged in optical heterodyne experiments, but to our knowledge, the general case has not. A derivation of this very useful result, modeled after one first given by H. Kogelnik, may be found in the appendix, which also contains other interesting applications of the general theorem.[8]

With no need to either carefully position the detector or require its surface to conform to the locus of the scanning beam waist, it can be located away from the focus, thereby reducing, by orders of magnitude, the peak instantaneous power densities at its surface. In addition, the effects of dust particles and other local anomalies of the detector surface are considerably reduced by an out-of-focus location. In all cases, the equivalent hologram is made at the locus of the scanning beam waist, independent of the actual detector position.

4.4 *Hologram Display and Recording*

The amplified and processed† output of the detector is used to intensity modulate a Westinghouse WX–30176P 10-inch high resolution kinescope. Synchronizing pulses from the optical deflectors are used to regenerate the sinusoidal sweeps necessary to match the kinescope sweeps to the optical ones. Because the horizontal and vertical optical deflection systems are both free-running oscillators, the kinescope display has random interlace. In conjunction with the several seconds of exposure required to record the kinescope output on Polaroid 46–L transparency film, this random interlace causes the scanning lines to be smeared together and undiscernible in the final hologram, eliminating the problem of diffraction by them.[9]

4.5 *Reconstruction*

The still limited resolution available with this system requires object-reference beam angles of less than 2°. To separate the real image from the direct beam and virtual image when reconstructing, the Fourier transform technique described by Enloe and others is used, the only modifications being the inclusion of cylindrical lenses in the final imaging process.[1] These permit compensation for astigmatic effects arising from both the oblique optical paths through the second beamsplitter and geometric distortions caused by disparities in the optical and electrical sweeps.

V. SIGNAL ENHANCEMENT TECHNIQUES

In addition to the desired signal [equation (7)] and shot noise [equation (8)], the detector output includes ac components due both to variations in the laser source output and position dependent modulations of the scanning beam. The largest of the source variations are periodic and result from plasma oscillations within the laser active medium. These are suppressed by the use of *rf* excitation of the discharge. The smaller, random, source fluctuations remaining, though comparable in amplitude with the desired signal, can be considerably attenuated by using two photodetectors in a balanced modulator configuration, as shown in Fig. 2. Source amplitude fluctuations, which produce in-phase variations in both photodetector outputs, are canceled in the following difference amplifier; the desired interference terms give rise to out-of-phase signals which are enhanced. As shown

† Various techniques for improving the signal-to-noise ratio which are used are discussed in the Section V.

in the appendix, this out-of-phase condition for the desired interference term can be assured only when using a lossless beamsplitter.

Position dependent modulations of the scanning beam are caused by dust and imperfections on the beamsplitter and detector surfaces as well as by multiple reflections. The poor impedance match between silicon and air causes particularly severe reflections at the detector surface. When conditions are right for this reflected light to be returned to the detector surface by a second reflection at some other optical surface, a modulation of the detector output in synchronism with the scanning spot position results. Either of these effects produce on the display kinescope a stationary pattern which can be distinguished from a true hologram by its presence in the absence of the object beam. Such position dependent modulations can be greatly attenuated by photographing the kinescope display with a double exposure technique: half of the necessary exposure is made in the usual way, while for the remainder the reference beam path is lengthened by a half wavelength and the gain of the final video amplifier is reversed in sign. This combination of optical and electrical phase shifts leaves unchanged those components of the video signal arising from interference between the object and reference beams, but reverses the polarity of the position dependent modulations described above. The position dependent modulations during the second exposure thus cancel those of the first, leaving only the desired object-reference beam interference terms.

The efficacy of these signal enhancement techniques is demonstrated in Fig. 3, which compares the outputs obtained using single detection, Fig. 3a, balanced detection, Fig. 3b, and balanced detection with double exposure, Fig. 3c. The presence of a significant amount of random noise, indicated by poor definition and contrast, is readily evident in Fig. 3a. The suppression of this noise by a balanced detection system yields considerable improvement, as shown by Fig. 3b. It is not possible, by inspection of Fig. 3b only, to determine whether or not any position dependent modulations are present. However, comparing it with Fig. 3c, in which they are suppressed, shows the nature and severity of their contribution.

VI. EXPERIMENTAL RESULTS

6.1 *Resolution*

When operated in the heterodyne mode, that is, with the off-axis reference beam simulated by a controlled frequency difference between

Fig. 3 — Effects of signal enhancement techniques on hologram quality: (a) single detection, (b) balanced detection, (c) balanced detection with phase-reversal and double exposure.

the object and on-axis reference beams, this system should produce holograms that yield reconstructions with resolutions equal to those obtainable when using the same deflection system as a conventional flying-spot scanner. This assumes that the kinescope-camera portion of the system has a resolution capability of at least twice that of the optical scanner.

How well this prediction is met can be seen by comparing Fig. 4a, a photograph of the kinescope display taken when operating the system as a flying-spot scanner, with Fig. 4b, the real image reconstruction of the same object made from a transmitted hologram. Calculations, based on the parameters of the optical deflection system used, predict a resolution capability of 200 line-pairs; this value is reached in the flying-spot display of Fig. 4a. The measured limiting resolution of Fig. 4b, though only 160 line-pairs, is considerably in excess of the theoretical maximum of 100 obtainable with nonheterodyne scanning.

Figure 4a also shows the ability of the random interlace, when used in conjunction with a long exposure, to reduce the visibility of the scanning lines; the 60 lines per frame would otherwise produce a very coarse raster. Figure 5 indicates the subjective quality of the reconstructions obtainable with this system.

6.2 *Transmission of Three-Dimensional Images*

Heretofore it has been tacitly assumed but not really required that the subjects be two-dimensional. Actually this assumption may be dropped and more complicated objects considered. The next step in complexity, the simplest three-dimensional scene, consists of two (two-dimensional) transparencies separated longitudinally. The hologram transmitted for such a three-dimensional "object" (a vertical grating of period 0.5 mm located 5 cm behind a transparency portrait) is shown in Fig. 6.

The necessarily nondiffuse nature of both the illumination and the subject transparencies used in this experiment results in an extremely limited field of view, preventing the use for depth cues of not only binocular vision but also parallax. Demonstration of the three-dimensional nature of the reconstruction obtained from this hologram is therefore limited to showing the optimum focus for different portions of the reconstruction to lie in different planes. The real image reconstruction from Fig. 6, when taken in the plane of best focus for the grating, is shown in Fig. 7a. Figure 7b shows the corresponding re-

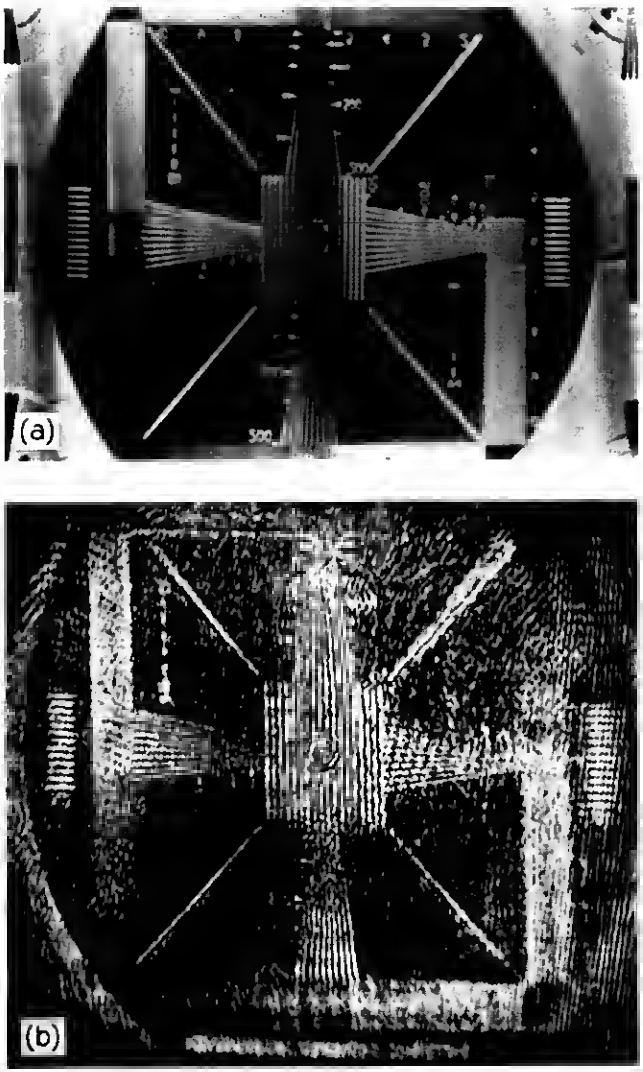

Fig. 4 — Comparison of image quality of flying-spot and heterodyne scanning transmissions: (a) flying spot, (b) heterodyne scanning.

Fig. 5 — Two-dimensional portrait reconstructed from transmitted hologram.

sult when the reconstructed image is recorded in that plane that provides optimum focus for the portrait, thus demonstrating the three-dimensional nature of the reconstructions obtainable with this system.

VII. SUMMARY AND CONCLUDING REMARKS

A heterodyne scanning system for transmitting holograms, which requires no camera tube and the theoretically minimum resolution from the optical deflectors, has been constructed. This required the development of a technique for obtaining two different but phase-related optical frequencies. Analyses have been made for the signal-to-noise ratio and resolution as functions of the system parameters, and the resolution predictions verified experimentally. Several techniques for improving the system signal-to-noise ratio have been implemented. The use of random interlace and many-field exposures avoided the problems of diffraction by the scanning lines when reconstructing. Off-axis holograms of both two- and three-dimensional objects have been transmitted and reconstructed.

The kinescope-camera receiving system, though easily implemented

in the laboratory, is not only limited in its resolution capability, but is also unsuited for real-time operation. However, a receiver operating on the Eidophor principle would not only solve the real-time problem but the resulting phase holograms would also provide increased optical efficiency in reconstruction.[10]

Because of its compatibility with other bandwidth reduction schemes, the heterodyne scanning technique should find application wherever holographic information is to be transmitted over systems having limited resolution or bandwidth. The present edge in resolution held by conventional camera tubes over optical scanning devices is expected to disappear as a result of the considerable effort now being applied to optical deflection techniques.

The experimental observation and subsequent proof that the detector output is independent of the position of the scanning beam waist relative to the detector should prove to be important not only to the successful operation of this experiment but to the extension of flying-spot scanning techniques into areas where depth of focus problems have heretofore prevented their application.

Concurrent with the submission of this paper and the publication

Fig. 6 — Hologram of three-dimensional scene.

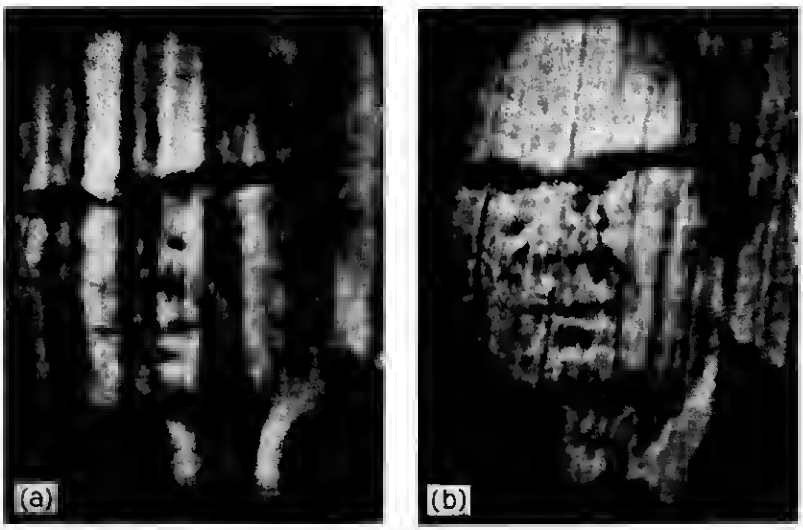

Fig. 7 — Demonstration of three-dimensional nature of image reconstructed from hologram shown in Fig. 6: (a) bars in optimum focus, (b) portrait in optimum focus.

of Ref. 3, Bertolotti and others published the results of their analysis and experiments on a one-dimensional holographic transmission system.[3,11] The transmitter described here, when operated in a non-heterodyne mode, is similar to theirs, but their analysis and proposed receiving system are different. The interested reader will find it worthwhile to become acquainted with their approach to the problem of hologram transmission.

VIII. ACKNOWLEDGMENTS

The author acknowledges fruitful discussions with L. H. Enloe, H. Kogelnik, R. C. Brainard, and C. B. Rubinstein.

APPENDIX

Conservation of Beat Energy

A.1 *Derivation*

We consider the limitations and conditions under which the beat signal obtained by detecting the interference between two optical beams is independent of the detector location. The analysis is modeled after one proposed by H. Kogelnik.[8]

Consider a volume containing no optical sources or sinks and having a boundary that is everywhere in free space. Under these conditions, Poynting's theorem for any incremental volume in this region can be written

$$\nabla \cdot \mathbf{S} + \frac{\partial W}{\partial t} = 0, \tag{14}$$

where $\mathbf{S} = \mathbf{E} \times \mathbf{H}$ and $W = \frac{1}{2}\epsilon E^2 + \frac{1}{2}\mu H^2$. $\mathbf{E}$ and $\mathbf{H}$, the resultant real electric and magnetic fields produced by the combination of the two beams, can be written as the sum of the single frequency real fields corresponding to each beam:

$$\begin{aligned} \mathbf{E} &= \mathbf{E}_1 \exp i\omega_1 t + \mathbf{E}_1^* \exp -i\omega_1 t \\ &\quad + \mathbf{E}_2 \exp i\omega_2 t + \mathbf{E}_2^* \exp -i\omega_2 t \\ \mathbf{H} &= \mathbf{H}_1 \exp i\omega_1 t + \mathbf{H}_1^* \exp -i\omega_1 t \\ &\quad + \mathbf{H}_2 \exp i\omega_2 t + \mathbf{H}_2^* \exp -i\omega_2 t, \end{aligned} \tag{15}$$

where ω_1 and ω_2 may or may not be equal. Substituting the values of $\mathbf{E}$ and $\mathbf{H}$ from equation (15) into equation (14), and comparing beat terms varying as $\exp i(\omega_1 - \omega_2)t$, we have

$$\nabla \cdot (\mathbf{E}_1 \times \mathbf{H}_2^* + \mathbf{E}_2^* \times \mathbf{H}_1) = -i(\omega_1 - \omega_2)(\epsilon \mathbf{E}_1 \cdot \mathbf{E}_2^* + \mu \mathbf{H}_1 \cdot \mathbf{H}_2^*). \tag{16}$$

Equation (16) rewritten in the integral form gives

$$\begin{aligned} &\oint_C (\mathbf{E}_1 \times \mathbf{H}_2^* + \mathbf{E}_2^* \times \mathbf{H}_1) \cdot d\mathbf{A} \\ &\qquad = -i(\omega_1 - \omega_2) \iiint_V (\epsilon \mathbf{E}_1 \cdot \mathbf{E}_2^* + \mu \mathbf{H}_1 \cdot \mathbf{H}_2^*)\, dV, \end{aligned} \tag{17}$$

where the surface C encloses the volume of integration V. A photodetector intercepting these fields will provide a beat signal current, I_b, having a complex amplitude given by

$$I_b = K \iint_D (\mathbf{E}_1 \times \mathbf{H}_2^* + \mathbf{E}_2^* \times \mathbf{H}_1) \cdot d\mathbf{A}, \tag{18}$$

where D is the area of the detector and K incorporates several physical constants. The left side of equation (17) is now recognized as giving, within a constant multiplier, the response of a detector intercepting all of the beat energy crossing surface C. For the case where $\omega_1 = \omega_2$, the right side of equation (17) is identically zero. Under appropriate condi-

tions, defined in Section A.3, it is possible for the right side to be negligible even with $\omega_1 \neq \omega_2$. The following three important results, derivable from this theorem assume a zero right side.

A.2 *Applications*

A.2.1 *Constancy of Detected Beat*

Consider, as shown in Fig. 8a, a volume through which the combined beams are propagating. Let C_1 contain all of the surface C common to the two beams as they propagate into the volume, and C_2 contain all of C common to the beams as they leave. Then, by definition, the vector product is zero everywhere except over some regions of C_1 and C_2, and equation (17) can be written

$$\iint_{C_1} (\mathbf{E}_1 \times \mathbf{H}_2^* + \mathbf{E}_2^* \times \mathbf{H}_1) \cdot d\mathbf{A} + \iint_{C_2} (\mathbf{E}_1 \times \mathbf{H}_2^* + \mathbf{E}_2^* \times \mathbf{H}_1) \cdot d\mathbf{A} = 0. \quad (19)$$

Taking into account the relative directions of the vector products and the surface normals at C_1 and C_2 leads to the conclusion that a detector intercepting the beams crossing C_2 yields identically the same output as a similar detector intercepting the beams crossing C_1. Since the separation of C_1 and C_2 is arbitrary, the detector output is independent of its location, provided all of the area common to both beams is intercepted.

A.2.2 *Phase Relationships with a Lossless Beamsplitter*

In the case shown in Fig. 8b, the surface C encloses a lossless beamsplitter which is combining two input beams into two output beams, each output containing a part of both inputs. C_1 and C_2 again contain all the portions of C that are common to both beams. As before, the cross-product is, by virtue of the definition of C_1 and C_2, zero everywhere except on C_1 and C_2, so that equation (19) still applies. However, when the relative directions of the beat energy flux and the surface normals are taken into account, we arrive at the result that the interaction at one detector must be the negative of that at the other, yielding detector outputs 180° out of phase.

A.2.3 *Combining Beams without a Beamsplitter*

The last case to be considered involves two otherwise separate beams brought in at appropriate angles so they overlap at the detector sur-

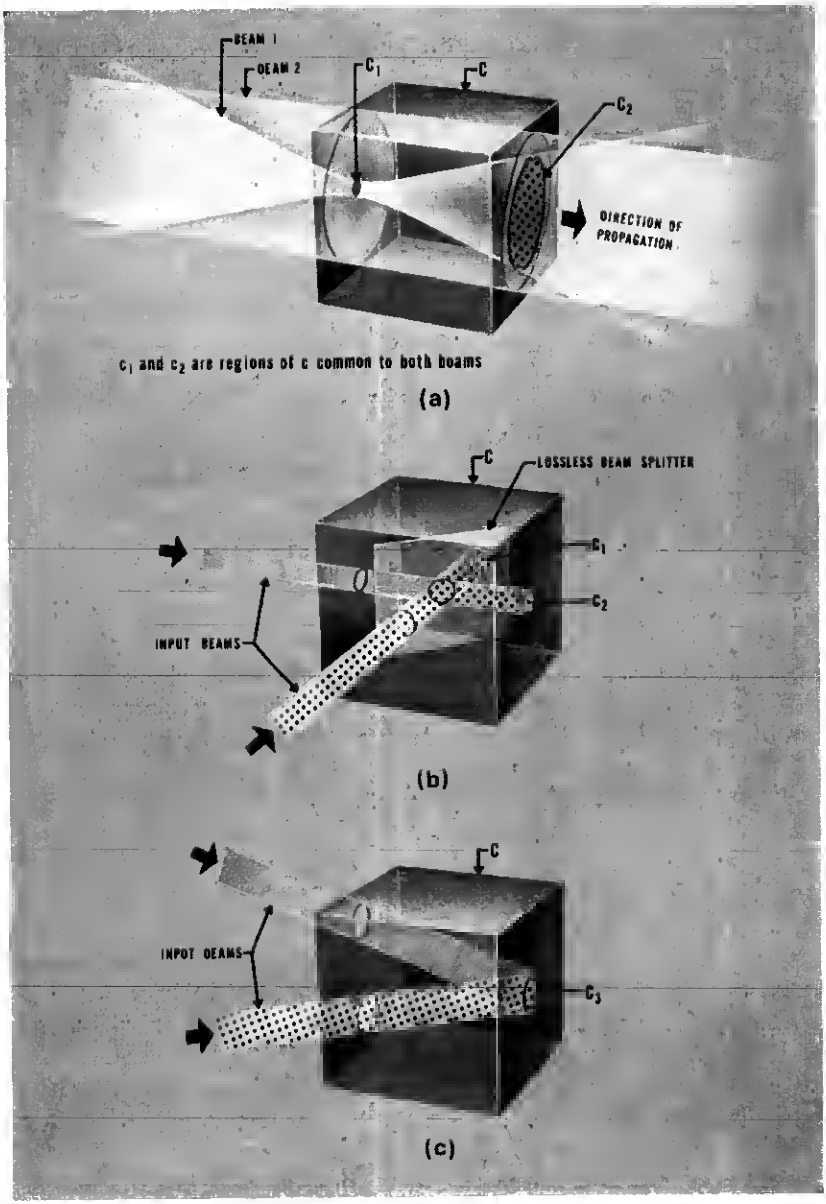

Fig. 8 — Applications of theorem on conservation of beat energy: (a) independence of detector position, (b) phase relationships with lossless beamsplitter, (c) combining beams without a beamsplitter.

face. As shown in Fig. 8c, the surface C is chosen in this case to pass just in front of the detector and to close in some region of space where the two beams are separate. Now the interaction term is everywhere zero on C except at C_3, where the two beams overlap. Equation (17) for this situation reduces to

$$\iint_{C_3} (\mathbf{E}_1 \times \mathbf{H}_2^* + \mathbf{E}_2^* \times \mathbf{H}_1) \cdot d\mathbf{A} = 0, \tag{20}$$

which says that no interference is detected in this arrangement. This identical result was derived in a completely different fashion in the body of the paper in connection with the analysis of the system resolution.

A.3 *Extensions and Limitations*

Notice that these derivations require absolutely no assumptions as to the structure of either of the fields other than that they obey Maxwell's equations. Furthermore, there are no restrictions on any distances involved.

For the beterodyne case where $\omega_1 - \omega_2 \neq 0$, equation (17) has a nonzero right side. However, for small heat frequencies the above rules are still true. Although evaluation of the right side of equation (17) for the general heterodyne case is impractical, a simple example can be analyzed to indicate when it may reasonahly he ignored.

Imagine a region of free space containing two plane waves with the same polarization but different frequencies, both propagating in the $+z$ direction. It can easily be shown that the single (z-directed) beat frequency component of the Poynting vector has an amplitude which is independent of z. However, its phase does vary with longitudinal position, changing by $\pi/2$ for every change in z of $\pi c/2(\omega_1 - \omega_2)$. For the 3-MHz beats observed in this experiment, this quarter-wave distance was 25 meters, much larger than the dimensions of the experimental apparatus. It is reasonable to assume that a similar phase variation would be found in the general case.

Altbough the amplitude of the interaction was constant even in the heterodyne case for the plane wave example, it can be shown to decrease with z for gaussian beams.[8] This amplitude change, however, typically occurs over distances orders of magnitude larger than that for the phase change; even for the extreme case of different wavelength gaussian beams focused by an $f/1$ optical system, significant phase variations of the detected heat signal occur with detector move-

ments an order of magnitude less than required for correspondingly significant amplitude changes.

REFERENCES

1. Enloe, L. H., Murphy, J. A., and Rubinstein, C. B., "Hologram Transmission via Television," B.S.T.J., *45*, No. 2 (February 1966), pp. 335–339.
2. Burckhardt, C. B. and Doherty, E. T., "Formation of Carrier Frequency Holograms with an On-Axis Reference Beam," Appl. Opt., *7*, No. 6 (June 1968), pp. 1191–1192.
3. Enloe, L. H., Jakes, W. C. Jr., and Rubinstein, C. B., "Hologram Heterodyne Scanners," B.S.T.J., *47*, No. 9 (November 1968), pp. 1875–1882.
4. Lin, L. H., "A Method of Hologram Information Reduction by Spatial Frequency Sampling," Appl. Opt., *7*, No. 3 (March 1968), pp. 545–548.
5. Haines, K. A. and Brumm, D. B., "Holographic Data Reduction," Appl. Opt., *7*, No. 6 (June 1968), pp. 1185–1189.
6. Born, M. and Wolf, E., *Principles of Optics*, New York: Pergamon Press, 1965, p. 396 and 398.
7. Gradshteyn, I. S. and Ryzhik, I. M., *Table of Integrals Series and Products*, New York: Academic Press, 1965, p. 667.
8. Kogelnik, H., unpublished work.
9. Klimenko, I. S. and Rukman, G. I., "Wavefront Reconstruction by Holograms Transmitted by Television," Zh. Tekh. Fiz., *37*, (August 1967), pp. 1532–1534. Translated in Sov. Phys.—Tech. Phys., *12*, No. 8 (February 1968), pp. 1115–1116.
10. Baumann, E., "The Fischer Large-Screen Projection System (Eidophor)," J. Soc. Motion Picture and Television Engineers, *60*, No. 4 (April 1953), pp. 344–356.
11. Bertolotti, M., Gori, F., Guattari, G., and Daino, B., "On a Method of Conversion and Reconversion of Spatial into Temporal Frequencies," Appl. Opt., *7*, No. 10 (October 1968), pp. 1961–1964.